Dynamic Intermittent Feedback Design for H_∞ Containment Control on a Directed Graph

Yongliang Yang, *Member, IEEE*, Hamidreza Modares, *Member, IEEE*, Kyriakos G. Vamvoudakis, *Senior Member, IEEE*, Yixin Yin, *Member, IEEE*, and Donald C. Wunsch, II, *Fellow, IEEE*

***Abstract*—This article develops a novel distributed intermittent control framework with the ultimate goal of reducing the communication burden in containment control of multiagent systems communicating via a directed graph. Agents are assumed to be under disturbance and communicate on a directed graph. Both static and dynamic intermittent protocols are proposed. Intermittent H_∞ containment control design is considered to attenuate the effect of the disturbance and the game algebraic Riccati equation (GARE) is employed to design the coupling and feedback gains for both static and dynamic intermittent feedback. A novel scheme is then used to unify continuous, static, and dynamic intermittent containment protocols. Finally, simulation results verify the efficacy of the proposed approach.**

***Index Terms*—Game algebraic Riccati equation (GARE), H_∞ intermittent containment control, multiagent systems (MASs).**

I. Introduction

COOPERATIVE behavior and multiagent systems (MASs) [1]–[3] have widespread applications, including microgrids [4] and social networks [5]. In distributed cooperative control of MAS, the control protocol for each agent depends only on neighborhood information, rather than the global information of the overall system, which might not be available. Agents exchange their information throughout a communication network to achieve a global group objective, such as formation and synchronization [6]. In an MAS setting with multiple leaders, namely, the containment control problem, the followers design their distributed control protocols so that their state or output falls into a convex hull spanned by the leaders [7], [8].

Existing solutions to the containment control problem [9], [10] require continuous interactions and information exchange amongst the agents which may not be efficient and doable when there are limited resources in terms of communication, energy, and bandwidth.

Related Work: Continuous state/output sampling can be problematic in the context of cyber-physical systems, where multiple and possibly remotely located plants, sensors, and actuators, communicate through a shared medium (e.g., wireless connections), making it crucial for resources, such as data, bandwidth, and energy to be used efficiently. Several real-time scheduling mechanisms have been developed to reduce the computational and the communication loads [11]–[18]. In such cases, the controller is only updated when a sampling error exceeds a certain threshold, to guarantee stability of the equilibrium point, while ensuring robustness and/or optimality. However, the dependency of each agent's update on the sampling of its neighbors may potentially increase further the communication and computation loads [19], [20]. Therefore, there is a need for a class of "combinative" measurements based on an intermittent feedback design.

Considering the dependency of the threshold on the state, Fan *et al.* [19] categorized the event-triggered conditions as state independent [21] and state dependent [22]. The threshold parameter is closely related to the communication load amongst the agents in the networks. In both cases, the threshold parameters are constant, and are referred to, as static intermittent mechanisms. However, it is not desirable to hold the threshold parameters constant, since they might exclude useful data transmissions [23]. Hence, there is a need for a more dynamic framework that leads to a time-varying threshold. Toward that goal, the work of [24] presented the concept of a dynamic intermittent feedback, wherein the intermittent condition is nonpositive only in an

Manuscript received March 6, 2019; revised June 16, 2019; accepted August 1, 2019. This work was supported in part by the National Natural Science Foundation of China under Grant 61903028 and Grant 61333002, in part by the Fundamental Research Funds for the China Central Universities of USTB under Grant FRFTP-18-031A1 and Grant FRF-BD-17-002A, in part by the China Post-Doctoral Science Foundation under Grant 2018M641197, in part by the National Science Foundation under Grant NSF CAREER CPS-1851588, in part by the Mary K. Finley Missouri Endowment, in part by the Missouri S&T Intelligent Systems Center, in part by the Lifelong Learning Machines program from DARPA/Microsystems Technology Office, and in part by the Army Research Laboratory under Agreement W911NF-18-2-0260. The views and conclusions contained in this document are those of the authors and should not be interpreted as representing the official policies, either expressed or implied, of the Army Research Laboratory or the U.S. Government. The U.S. Government is authorized to reproduce and distribute reprints for Government purposes notwithstanding any copyright notation herein. This article was recommended by Associate Editor H. Zhang. *(Corresponding author: Yongliang Yang.)*

Y. Yang and Y. Yin are with the School of Automation and Electrical Engineering, University of Science and Technology Beijing, Beijing 100083, China, and also with the Key Laboratory of Knowledge Automation for Industrial Processes, Ministry of Education, Beijing 100083, China (e-mail: yangyongliang@ieee.org; yyx@ies.ustb.edu.cn).

H. Modares is with the Mechanical Engineering Department, Michigan State University, East Lansing, MI 48824 USA (e-mail: modaresh@msu.edu).

K. G. Vamvoudakis is with the Daniel Guggenheim School of Aerospace Engineering, Georgia Tech, GA 30332 USA (e-mail: kyriakos@gatech.edu).

D. C. Wunsch, II, is with the Department of Electrical and Computer Engineering, Missouri University of Science and Technology, Rolla, MO 65401 USA (e-mail: dwunsch@mst.edu).

Color versions of one or more of the figures in this article are available online at http://ieeexplore.ieee.org.

Digital Object Identifier 10.1109/TCYB.2019.2933736

average sense and shows that it can outperform the conventional static intermittent feedback in terms of the data transmission rate.

The presence of external disturbances and unmodeled dynamics in an MAS with multiple leaders might potentially degrade the performance of the corrupted agent, as well as the agents that are reachable from it [25]. The event-based containment control design for MAS with simple linear dynamics has been considered in [26] and [27]. However, the effect of a disturbance input on the performance has not been considered yet. This article investigates the intermittent feedback design for H_∞ containment control problem for general high-order linear dynamics. Existing Lyapunov function designs for distributed control depend heavily on the topology connectivity, such as strongly connected graph [28] and strongly connected and detailed balanced graph [29]. In addition, multiple leaders in containment control of MAS further increase the difficulty for proper Lyapunov function design. In this article, a proper Lyapunov function design is designed for the containment control problem to avoid unnecessary strong graph requirement.

Contributions: The contributions of this article are threefold. First, an amalgamated measurement-based intermittent containment control framework is developed. Second, it is shown that the presented intermittent protocol solves the containment control problem with a guaranteed H_∞ performance. Finally, a unified framework that combines the static, and the dynamic intermittent feedback is presented to further decrease the data transmission rate amongst the agents while excluding Zeno behavior.

Structure: The remainder of this article is structured as follows. Section II formulates the containment control problem for leader–follower MAS of general high-order linear dynamics with disturbances. To avoid the continuous interaction amongst the agents, Section III develops an aperiodic and asynchronous sampling scheme for the containment error, namely, a novel static intermittent containment control protocol. To further reduce the state sampling frequency, Section IV provides a novel dynamic intermittent scheme. A simulation example is shown in Section V to validate the efficiency of the presented approach. Finally, Section VI provides the conclusion and discusses future research directions.

Notation: The following notations are needed.

$\otimes$ $\triangleq$ Kronecker product.
$\bar{\lambda}(\mathcal{M})$ $\triangleq$ maximum eigenvalue of matrix $\mathcal{M}$.
$\underline{\lambda}(\mathcal{M})$ $\triangleq$ minimum eigenvalue of matrix $\mathcal{M}$.
$\mathcal{G}$ $\triangleq$ $\{1, \dots, M+N\}$, the set of all agents.
$\mathcal{R}$ $\triangleq$ $\{1, \dots, M\}$, the set of leaders.
$\mathcal{F}$ $\triangleq$ $\{M+1, \dots, M+N\}$, the set of followers.
$\mathcal{N}_i$ $\triangleq$ set of neighbors of the ith follower.
$\mathcal{A}$ $\triangleq$ adjacency matrix of subgraph $\mathcal{F}$.
a_{ij} $\triangleq$ (i,j)th entry of adjacency matrix $\mathcal{A}$, $a_{ij} = 1$ if there exists connection from ith to jth follower; otherwise, $a_{ij} = 0$.
d_i $\triangleq$ $\sum_{j\in\mathcal{F}} a_{ij}$, the in-degree of the ith follower.
$\mathcal{D}$ $\triangleq$ $\mathrm{diag}\{d_1, \dots, d_N\}$, the in-degree matrix of the subgraph $\mathcal{F}$.
$\mathcal{L}$ $\triangleq$ $\mathcal{D} - \mathcal{A}$, the Laplacian matrix of subgraph $\mathcal{F}$.
g_i^l $\triangleq$ pinning gain from the lth leader to the ith follower $g_i^l = 1$ if ith follower is connected to the lth leader; otherwise, $g_i^l = 0$.
G_l $\triangleq$ $\mathrm{diag}\{g_1^l, \dots, g_N^l\}$, the pinning matrix of the lth leader to all followers.
G $\triangleq$ $\sum_{l\in\mathcal{R}} G_l$, pinning matrix from leaders set $\mathcal{R}$ to followers set $\mathcal{F}$.
g_i $\triangleq$ $\sum_{l\in\mathcal{R}} g_i^l$, the ith element on the diagonal of G.
h_l $\triangleq$ $\mathcal{L}/_M + G_l \in \mathbb{R}^{N\times N}$.
h $\triangleq$ $\mathcal{L} + G \in \mathbb{R}^{N\times N}$, of which the (i,j)th entry is denoted as h_{ij}.
H_l $\triangleq$ $h_l \otimes I_n \in \mathbb{R}^{nN\times nN}$.
H $\triangleq$ $h \otimes I_n \in \mathbb{R}^{nN\times nN}$.
$\mathbf{1}_N$ $\triangleq$ N-dimensional column vector with all entries as 1.
I_n $\triangleq$ n-dimensional identity matrix.

Definition 1 (Convex Hull [30]): A set $\mathcal{C} \subseteq \mathbb{R}^n$ is convex if $(1-\alpha)x + \alpha y \in \mathcal{C}, \forall x, y \in \mathcal{C}$ and $\forall \alpha \in [0, 1]$. The convex hull $Co(\mathcal{X})$ of a finite set of points $\mathcal{X} = \{x_1, x_2, \dots, x_p\}$ is the minimal convex set containing all points in $\mathcal{X}$. That is, $Co(\mathcal{X}) = \{\sum_{l=1}^{p} \alpha_l x_l | x_l \in \mathcal{X}, \alpha_l \geq 0 \sum_{l=1}^{p} \alpha_l = 1.\}$.

Definition 2 (Distance [30]): Let $x \in \mathbb{R}^n$ and $\mathcal{C} \subseteq \mathbb{R}^n$. Then, the distance from x to the set $\mathcal{C}$ is defined as

$$\mathrm{dist}(x, \mathcal{C}) = \inf_{y\in\mathcal{C}} \|x - y\|.$$

II. Problem Formulation

Consider the dynamics of the M uncontrolled leaders

$$\dot{x}_l = Ax_l,\ l \in \mathcal{R},\ t \geq 0 \tag{1}$$

where $x_l \in \mathbb{R}^n$ is the leader's state vector. Let $\bar{x}_l = \mathbf{1}_N \otimes x_l$, $\forall l \in \mathcal{R}$. Then, for each leader, one has

$$\dot{\bar{x}}_l(t) = (I_N \otimes A)\bar{x}_l(t),\ t \geq 0. \tag{2}$$

Consider the dynamics of the N followers, given as

$$\dot{x}_i = Ax_i + B_1 u_i + B_2 w_i, i \in \mathcal{F}, t \geq 0 \tag{3}$$

where $x_i \in \mathbb{R}^n$ is the state vector, $u_i \in \mathbb{R}^{m_1}$ is the control input, and $w_i \in \mathbb{R}^{m_2}$ is a disturbance input.

Assumption 1 [3]: The subgraph $\mathcal{F}$ is directed, and for each follower, there exists at least one leader that has a directed path to it. That is, the graph $\mathcal{G}$ has a united directed spanning tree.

The following lemma adopted from [31] and [32] shows some important properties that we will use throughout this article.

Lemma 1: Under Assumption 1, let $\xi = h^{-T}\mathbf{1}_N$, $\Xi = \mathrm{diag}(\xi) \in \mathbb{R}^{N\times N}$, and $\Omega = \Xi h + h^T \Xi \in \mathbb{R}^{N\times N}$. Then:

1) $\Xi \succ 0$ and $\Omega \succ 0$;
2) $\Omega \geq \lambda_0 \Xi$ with $\lambda_0 = \underline{\lambda}(h + \Xi^{-1} h^T \Xi)$.[1]

[1]In this article, the notation of $\mathcal{M}_1 \geq (\succ) \mathcal{M}_2$ for symmetric matrices $\mathcal{M}_1$ and $\mathcal{M}_2$ is equivalent to $\mathcal{M}_1 - \mathcal{M}_2 \geq (\succ) 0$.

Assumption 2: The pair (A, B_1) is stabilizable.

Define the disagreement vector $\delta_i \in \mathbb{R}^n$ for $i \in \mathcal{F}$ as

$$\delta_i \triangleq \sum_{j\in\mathcal{N}_i} a_{ij}\big(x_i - x_j\big) + \sum_{l\in\mathcal{R}} g_i^l (x_i - x_l). \tag{4}$$

By augmenting (4) for all the followers, we can write the global disagreement as

$$\delta = Hx - \sum_{l\in\mathcal{R}} H_l \bar{x}_l \tag{5}$$

where

$$x := \begin{bmatrix} x_{M+1}^T & \cdots & x_{M+N}^T \end{bmatrix}^T \in \mathbb{R}^{nN}$$
$$\delta := \begin{bmatrix} \delta_{M+1}^T & \cdots & \delta_{M+N}^T \end{bmatrix}^T \in \mathbb{R}^{nN}.$$

Based on (2) and (4), and after taking the time derivative of δ_i, one has

$$\begin{aligned}\dot{\delta}_i &= A\left(\sum_{j\in\mathcal{N}_i} a_{ij}\big(x_i - x_j\big) + \sum_{l\in\mathcal{R}} g_i^l (x_i - x_l)\right)\\ &\quad + B_1\left[\left(\sum_{j\in\mathcal{N}_i} a_{ij} + \sum_{l\in\mathcal{R}} g_i^l\right)u_i - \sum_{j\in\mathcal{N}_i} a_{ij}u_j\right]\\ &\quad + B_2\left[\left(\sum_{j\in\mathcal{N}_i} a_{ij} + \sum_{l\in\mathcal{R}} g_i^l\right)w_i - \sum_{j\in\mathcal{N}_i} a_{ij}w_j\right]\\ &= A\delta_i + \sum_{j\in\mathcal{F}} h_{ij}B_1u_j + \sum_{j\in\mathcal{F}} h_{ij}B_2w_j \qquad (6)\\ \dot{\delta} &= (I_N \otimes A)\delta + (h\otimes B_1)u + (h\otimes B_2)w \qquad (7)\end{aligned}$$

where h_{ij} is the (i, j)th entry of matrix h satisfying

$$h_{ii} = \sum_{j\in\mathcal{N}_i} a_{ij} + \sum_{l\in\mathcal{R}} g_i^l,\ h_{ij} = -a_{ij}$$

with

$$u = \begin{bmatrix} u_{M+1}^T & \cdots & u_{M+N}^T \end{bmatrix}^T \in \mathbb{R}^{nN}$$
$$w = \begin{bmatrix} w_{M+1}^T & \cdots & w_{M+N}^T \end{bmatrix}^T \in \mathbb{R}^{nN}.$$

Remark 1: In this article, we consider general linear systems where the full state information is available for feedback. This is applicable to the single-integrator agent if one can measure the position and the double-integrator agent if one can measure both the position and velocity. In the case that the full state is not available, one can add an observer to estimate the state of each agent and extend the framework to output feedback by following [33] and [34]. Moreover, in directed graphs, the requirement of existence of a directed spanning tree is weaker than the requirement of having a strongly connected graph [3]. Assumption 1 further relaxes the requirement of the followers subgraph $\mathcal{F}$ containing a spanning tree and hence it is only required that the augmented graph $\mathcal{G}$ has a united spanning tree.

Problem 1 (H_∞ Containment Control): Consider the MASs with leaders given by (1) and followers given by (3). For a prescribed attenuation level $\gamma > 0$, design the distributed protocols u_i for each follower $i \in \mathcal{F}$ such that:

1) all the followers are synchronized to the convex hull spanned by the leaders when $w(t) = 0$, that is
$$\lim_{t\to\infty} \operatorname{dist}\big(x_i(t), \operatorname{Co}\{x_l(t)\}_{l\in R}\big) = 0, \forall i \in \mathcal{F}$$
2) under zero-initial conditions $\delta_i = 0,\ \forall i$, the $\mathcal{L}_2$-gain condition for the system described in (7) is satisfied $\forall w \in \mathcal{L}_2[0, \infty)$, that is
$$\int_0^\infty \delta^T\delta \mathrm{d}\tau \le \gamma^2 \int_0^\infty w^T w \mathrm{d}\tau. \tag{8}$$

As shown in [7] and [8], the first condition in Problem 1 is guaranteed if and only if the system (7) has an asymptotically stable equilibrium point, that is, $\delta = 0$. Therefore, δ and δ_i are referred to as global and local containment errors, respectively.

A. Continuous Feedback for the H_∞ Containment Control Design

Using (4), a distributed continuous-sampling-based containment control protocol is designed as

$$u_i = cK\delta_i,\ \ \forall i \in \mathcal{F} \tag{9}$$

where $c \in \mathbb{R}^+$ is the coupling gain and $K \in \mathbb{R}^{m_1\times n}$ is the feedback gain matrix to be designed later.

The following theorem provides a solution to the continuous feedback containment control design for Problem 1.

Theorem 1: Under Assumptions 1 and 2, Problem 1 is solved with a controller given by (9) given that, the parameters c and K are selected as

$$c \ge \frac{1}{\lambda_0}, K = -B_1^T P \tag{10}$$

where $P \succ 0$ is the unique solution to the following game algebraic Riccati equation (GARE):

$$A^T P + PA + Q + \frac{1}{\gamma^2} PB_2B_2^T P - PB_1B_1^T P = 0 \tag{11}$$

where $Q \triangleq qI_n \succ 0, q \in \mathbb{R}^+$ and the pair $(A, \sqrt{Q})$ being detectable.

Proof: Substituting the distributed protocol (9) into (6) and (7), one has

$$\dot{\delta} = (I_N \otimes A)\delta + (ch\otimes B_1K)\delta + (h\otimes B_2)w. \tag{12}$$

1) We first consider the stability of the equilibrium point $\delta_i = 0$ of system (12) for the case that $w_i = 0, \forall i \in \mathcal{F}$.

Consider the Lyapunov candidate $V(\delta) = (1/2)\delta^T(\Xi\otimes P)\delta$, where Ξ is defined in Lemma 1 and P is the solution to the GARE given in (11). Since $(A, \sqrt{Q})$ is delectable and (A, B_1) is stabilizable, then P is positive definite. Therefore, $\Xi\otimes P$ is positive definite. Differentiating V along the error dynamics given in (12), one can obtain

$$\begin{aligned}\dot{V} &= \frac{1}{2}\delta^T(\Xi\otimes P)\dot{\delta} + \frac{1}{2}\dot{\delta}^T(\Xi\otimes P)\delta\\ &= \frac{1}{2}\delta^T(\Xi\otimes P)[(I_N\otimes A)\delta + (\mathrm{ch}\otimes B_1K)\delta]\\ &\quad + \frac{1}{2}[(I_N\otimes A)\delta + (\mathrm{ch}\otimes B_1K)\delta]^T(\Xi\otimes P)\delta.\end{aligned}$$

$$\mathcal{H} \leq L\left(\delta^T\delta - \gamma^2 w^T w\right) + \frac{1}{2}\delta^T(\Xi \otimes P)(h \otimes B_2)w + \frac{1}{2}w^T\left(h^T \otimes B_2^T\right)(\Xi \otimes P)\delta - \frac{1}{2}\delta^T\left[\Xi \otimes \left(Q + \frac{1}{\gamma^2}PB_2^TB_2P\right)\right]\delta$$
$$= \underbrace{\begin{bmatrix} (I_N \otimes B_2P)\delta \\ (\Xi h \otimes I_n)w \end{bmatrix}^T \begin{bmatrix} -\frac{1}{2\gamma^2}[\Xi \otimes I_n] & \frac{1}{2}I_N \otimes I_n \\ \frac{1}{2}I_N \otimes I_n & -L\gamma^2\left(\Xi^{-1}h^{-T}h^{-1}\Xi^{-1} \otimes I_n\right) \end{bmatrix} \begin{bmatrix} (I_N \otimes B_2P)\delta \\ (\Xi h \otimes I_n)w \end{bmatrix}}_{\bar{\mathcal{H}}} + \sum_{i \in \mathcal{F}}\left(L - \frac{q\xi_i}{2}\right)\delta_i^T\delta_i \quad (15)$$

Using the feedback $K = -B_1^TP$ yields

$$\dot{V} = \delta^T\left(\Xi \otimes \frac{PA + A^TP}{2}\right)\delta - \delta^T\left(\frac{c\left(\Xi h + h^T\Xi\right)}{2} \otimes PB_1B_1^TP\right)\delta.$$

Let $\Omega := \Xi h + h^T\Xi \in \mathbb{R}^{N\times N}$, then

$$\dot{V} = \delta^T\left(\Xi \otimes \frac{PA + A^TP}{2}\right)\delta - \frac{c}{2}\delta^T\left[\Omega \otimes PB_1B_1^TP\right]\delta.$$

According to Lemma 1, one has $\Omega \geq \lambda_0\Xi$ with $\lambda_0 = \underline{\lambda}(h + \Xi^{-1}h^T\Xi)$. Then, (10) guarantees that

$$\frac{c}{2}\delta^T\left[-\Omega \otimes PB_1B_1^TP\right]\delta \leq \frac{c}{2}\delta^T\left[-\lambda_0\Xi \otimes PB_1B_1^TP\right]\delta \leq -\frac{1}{2}\delta^T\left[\Xi \otimes PB_1B_1^TP\right]\delta. \quad (13)$$

Based on (10) and (11), one has

$$\dot{V} \leq -\frac{1}{2}\delta^T\left[\Xi \otimes \left(qI_n + \frac{1}{\gamma^2}PB_2B_2^TP\right)\right]\delta < 0. \quad (14)$$

2) Now consider the case that $w_i \neq 0$, and after differentiating V along the dynamics of (12), one can obtain

$$\dot{V} \leq \frac{1}{2}\delta^T(\Xi \otimes P)(h \otimes B_2)w + \frac{1}{2}w^T\left(h^T \otimes B_2^T\right)(\Xi \otimes P)\delta + \delta^T\left(\Xi \otimes \frac{PA + A^TP}{2}\right)\delta - \frac{c}{2}\delta^T\left[\Omega \otimes PB_1B_1^TP\right]\delta.$$

Based on (14), we can further write

$$\dot{V} \leq \frac{1}{2}\delta^T(\Xi \otimes P)(h \otimes B_2)w + \frac{1}{2}w^T\left(h^T \otimes B_2^T\right)(\Xi \otimes P)\delta - \frac{1}{2}\delta^T\left[\Xi \otimes \left(Q + \frac{1}{\gamma^2}PB_2B_2^TP\right)\right]\delta.$$

Consider now the Hamiltonian $\mathcal{H} := \dot{V} + L(\delta^T\delta - \gamma^2w^Tw)$ that formulates the H_∞ control problem, which can also be described by a zero-sum game where the controller acts as a minimizing player and the disturbance acts as the maximizing one. Then, $\mathcal{H}$ satisfies (15) (see the top of this page). To guarantee that $\mathcal{H} < 0$, the following conditions should be satisfied:

$$L - \frac{q\xi_i}{2} < 0, \quad \forall i \in \mathcal{F}$$
$$\begin{bmatrix} -\frac{1}{2\gamma^2}(\Xi \otimes I_n) & \frac{1}{2}I_N \otimes I_n \\ \frac{1}{2}I_N \otimes I_n & -L\gamma^2\left(\Xi^{-1}h^{-T}h^{-1}\Xi^{-1} \otimes I_n\right) \end{bmatrix} \prec 0.$$

Applying now the Schur complement lemma [35] yields

$$-\frac{1}{2\gamma^2}(\Xi \otimes I_n) \prec 0$$
$$-L\gamma^2\left(\Xi^{-1}h^{-T}h^{-1}\Xi^{-1} \otimes I_n\right) + \left[\frac{1}{2}I_N \otimes I_n\right]\left[\frac{1}{2\gamma^2}(\Xi \otimes I_n)\right]^{-1}\left[\frac{1}{2}I_N \otimes I_n\right] \prec 0. \quad (16)$$

The first matrix inequality in (16) can be guaranteed if $\Xi \succ 0$, which is shown in Lemma 1. The second matrix inequality in (16) holds if

$$L > \frac{1}{2}\xi_{\max}\bar{\lambda}\left(hh^T\right).$$

Therefore, L is selected as

$$\frac{1}{2}\xi_{\max}\bar{\lambda}\left(hh^T\right) < L < \frac{q\xi_i}{2} \quad (17)$$

with $\xi_{\max} = \max_{i\in\mathcal{F}}\xi_i$. Condition (17) eventually guarantees

$$\mathcal{H} = \dot{V} + L\left(\delta^T\delta - \gamma^2w^Tw\right) < 0.$$

Integrating now over $(0, t)$ yields

$$\int_0^t \delta_i^T\delta_i \mathrm{d}\tau - \int_0^t \gamma^2 w_i^T w_i \mathrm{d}\tau + \delta^T(t)(\Xi \otimes P)\delta(t) - \delta^T(0)(\Xi \otimes P)\delta(0) < 0.$$

Recall that $\delta_i(0) = 0$ $\forall i \in \mathcal{F}$, and $\Xi \otimes P$ is positive definite. Then, one can finally obtain

$$\int_0^\infty \delta_i^T\delta_i \mathrm{d}\tau \leq \int_0^\infty \gamma^2 w_i^T w_i \mathrm{d}\tau.$$

■

Remark 2: The results in this article can be extended to more complex cases. First, when the leader is driven by a bounded control input, then a discontinuous adaptive control method [8] and a continuous adaptive control using a boundary layer technique [36] can be used to compensate for that. Second, in the case that the followers have norm-bounded parameter uncertainties, one can use linear matrix inequality techniques to design the distributed containment control protocol as has been done in [37].

III. Static Intermittent Distributed H_∞ Containment Control Design

A. Static Intermittent Feedback Design

To efficiently utilize the limited resources in terms of bandwidth, and decrease the communication burden, a novel distributed intermittent mechanism is developed. This section designs a static intermittent control mechanism to solve

This article has been accepted for inclusion in a future issue of this journal. Content is final as presented, with the exception of pagination.

Problem 1. To this end, the control protocol for every follower $i \in \mathcal{F}$ is executed only when an event is triggered to guarantee stability of the equilibrium point and a desired performance level. That is, the local containment error remains constant between two successive events as follows:

$$\hat{\delta}_i(t) = \begin{cases} \delta_i(t_k^i), & \forall t \in \left[t_k^i, t_{k+1}^i\right) \\ \delta_i(t), & t = t_{k+1}^i \end{cases} \forall i \in \mathcal{F} \tag{18}$$

where $\{t_k^i\}_{k=0}^{\infty}$ is a monotonically increasing sequence of sampling instants, satisfying $\lim_{k\to\infty} t_k^i = \infty$, with $t_0^i = t_0\ \forall i \in \mathcal{F}$. Let $e_i(t)$ denotes the sampling error between $\hat{\delta}_i(t)$ and $\delta_i(t)$, that is

$$e_i(t) = \hat{\delta}_i(t) - \delta_i(t), \forall i \in \mathcal{F}. \tag{19}$$

Then, the intermittent control protocol can be designed, $\forall i \in \mathcal{F}$, as

$$u_i(t) = cK\hat{\delta}_i(t) = cK[e_i(t) + \delta_i(t)], t \in \left[t_k^i, t_{k+1}^i\right). \tag{20}$$

Substituting now the intermittent control given in (20) into (7) yields

$$\dot{\delta} = (I_N \otimes A + \mathrm{ch} \otimes B_1K)\delta + (\mathrm{ch} \otimes B_1K)e + (h \otimes B_2)w \tag{21}$$

where $e := [\, e_{M+1}^T \quad \cdots \quad e_{M+N}^T \,]^T$.

The following theorem provides a static intermittent containment control protocol design for solving Problem 1.

Theorem 2: Suppose that Assumptions 1 and 2 hold. Let the parameters c and K in (20) be selected as

$$c \geq \frac{1}{\lambda_0}, K = -B_1^T P \tag{22}$$

where $P \succ 0$ is the unique solution to the GARE (11) with $Q \triangleq qI_n \succ 0$, $\gamma_1 \triangleq \|PB_1B_1^TP\|$, and $\gamma_2 \triangleq \|PB_2B_2^TP\|$, and the pair $(A, \sqrt{Q})$ being detectable.

Moreover, suppose that the instants $\{t_k^i\}_{k=0}^{\infty}$ are determined by the following triggering condition:

$$\|e_i\| \geq \pi_i\|\delta_i\| \tag{23}$$

where

$$\pi_i = \sqrt{\frac{4r\sigma_i}{\bar{c}\gamma_1}\left(\frac{q\xi_i}{2} - L - \frac{\bar{c}\gamma_1 r}{4}\right)} \tag{24}$$

$$0 < r < \frac{4}{\bar{c}\gamma_1}\left(\frac{q\xi_{\min}}{2} - L\right) \tag{25}$$

$$0 < \sigma_i < \min\left\{\left(\frac{\bar{c}\gamma_1}{q\xi_{\max} - 2L}\right)^2, 1\right\} \tag{26}$$

with $\bar{c} = c\bar{\lambda}(\Omega)$, and L satisfying (17). Then, Problem 1 is solved by the intermittent protocol (20) with the triggering condition (23).

Proof: 1) We first consider the closed-loop stability of system (21) when $w_i = 0$, $\forall i \in \mathcal{F}$. Consider the Lyapunov candidate, $V(\delta) = (1/2)\delta^T(\Xi \otimes P)\delta$, for the global containment error δ. Taking the time derivative of V and substituting (21) yields

$$\begin{aligned} \dot{V} &= V_1 + V_2 \\ V_1 &= \delta^T\left(\Xi \otimes \frac{PA + A^TP}{2}\right)\delta - \frac{c}{2}\delta^T\left[\Omega \otimes PB_1B_1^TP\right]\delta \\ V_2 &= -\frac{c}{2}e^T\left[\Omega \otimes PB_1B_1^TP\right]\delta. \end{aligned} \tag{27}$$

From (13), (14), and (22), one has

$$\begin{aligned} V_1 &\leq -\frac{1}{2}\delta^T\left[\Xi \otimes \left(qI_n + \frac{1}{\gamma^2}PB_2B_2^TP\right)\right]\delta \\ &= -\frac{1}{2}\sum_{i\in\mathcal{F}}\xi_i\left(q + \frac{\gamma_2}{\gamma^2}\right)\|\delta_i\|^2 \triangleq \bar{V}_1. \end{aligned} \tag{28}$$

Note that the matrix Ω is symmetric and hence can be diagonalized. Consider now the orthogonal matrix $U^T = U^{-1}$ such that

$$\Lambda = U^T\Omega U, \Omega = U\Lambda U^T \tag{29}$$

where $\Lambda = \mathrm{diag}\{\lambda_i\}$ with $\{\lambda_i\}$ being the eigenvalues of matrix Ω. Then, the variable transformation can be accordingly defined as

$$\bar{e} = (U \otimes I_n)e, \bar{\delta} = (U \otimes I_n)\delta. \tag{30}$$

Applying now the Young's inequality to V_2 yields

$$\begin{aligned} V_2 &= -\frac{c}{2}\bar{e}^T\left[\Lambda \otimes PB_1B_1^TP\right]\bar{\delta} \\ &= -\frac{c}{2}\sum_{i\in\mathcal{F}}\lambda_i\bar{e}_i^TPB_1B_1^TP\bar{\delta}_i \\ &\leq \frac{\gamma_1}{4}\sum_{i\in\mathcal{F}}c\lambda_i\left(\frac{\|\bar{e}_i\|^2}{r} + r\left\|\bar{\delta}_i\right\|^2\right) \\ &\leq \frac{\gamma_1\bar{c}}{4}\sum_{i\in\mathcal{F}}\left[\frac{\|\bar{e}_i\|^2}{r} + r\left\|\bar{\delta}_i\right\|^2\right] \end{aligned}$$

where $\gamma_1 = \|PB_1B_1^TP\|$, and r is determined by (25). From (30), one has that

$$\bar{e}^T\bar{e} = e^Te, \bar{\delta}^T\bar{\delta} = \delta^T\delta. \tag{31}$$

Substituting (31) into V_2 yields

$$V_2 \leq \frac{\gamma_1\bar{c}}{4}\sum_{i\in\mathcal{F}}\left[\frac{\|e_i\|^2}{r} + r\|\delta_i\|^2\right] \triangleq \bar{V}_2. \tag{32}$$

From (28) and (32), one has

$$\begin{aligned} \dot{V} &\leq \bar{V}_1 + \bar{V}_2 \\ &= -\frac{1}{2}\sum_{i\in\mathcal{F}}\xi_i\left(q + \frac{\gamma_2}{\gamma^2}\right)\|\delta_i\|^2 + \frac{\gamma_1\bar{c}}{4}\sum_{i\in\mathcal{F}}\left(\frac{\|e_i\|^2}{r} + r\|\delta_i\|^2\right) \\ &= \sum_{i\in\mathcal{F}}\left\{\left[\frac{\bar{c}\gamma_1 r}{4} - \frac{\xi_i}{2}\left(q + \frac{\gamma_2}{\gamma^2}\right)\right]\|\delta_i\|^2 + \frac{\bar{c}\gamma_1}{4r}\|e_i\|^2\right\} \end{aligned} \tag{33}$$

where $\gamma_2 = \|PB_2B_2^TP\|$ and r is selected to guarantee that

$$G_i = \frac{\xi_i}{2}\left(q + \frac{\gamma_2}{\gamma^2}\right) - \frac{\bar{c}\gamma_1 r}{4} > 0, \forall i \in \mathcal{F}. \tag{34}$$

Then, the event is triggered as long as, for $\sigma_i \in (0, 1)$

$$\frac{\bar{c}\gamma_1}{4rG_i}\|e_i\|^2 \leq \sigma_i\|\delta_i\|^2 \tag{35}$$

is violated, which can be rewritten as

$$\|e_i\| \leq \rho_i\|\delta_i\|, \rho_i = \sqrt{\frac{4\sigma_i r}{\bar{c}\gamma_1}G_i}. \tag{36}$$

Denote $g_i = \sigma_i\|\delta_i\|^2 - [(\bar{c}\gamma_1)/(4rG_i)]\|e_i\|^2$, then, from (33), one has

$$\begin{aligned}\dot{V} &\leq \sum_{i\in\mathcal{F}}\left\{-(1-\sigma_i+\sigma_i)G_i\|\delta_i\|^2 + \frac{\bar{c}\gamma_1}{4r}\|e_i\|^2\right\}\\ &= \sum_{i\in\mathcal{F}}\left\{-(1-\sigma_i)G_i\|\delta_i\|^2 - G_i g_i\right\}\\ &\leq \sum_{i\in\mathcal{F}}\left\{-(1-\sigma_i)G_i\|\delta_i\|^2\right\} \leq 0 \end{aligned}\tag{37}$$

if $g_i \geq 0$ is guaranteed. From (37), one can observe that $\dot{V} = 0$ only if $\delta_i = 0$. Applying the LaSalle's theorem for nonsmooth systems [38, Th. 3.2] we obtain $\delta_i(t) \to 0$ for $i \in \mathcal{F}$ as $t \to \infty$, which guarantees that the containment is achieved [7].

2) Next, we analyze the $\mathcal{L}_2$-gain of the system given in (21). First, consider the variable transformation in (30) and the matrix transformation in (29). Then, differentiating V along (21) with $w \neq 0$ yields

$$\dot{V} = V_1 + V_2 + V_3 \tag{38}$$

where V_1 and V_2 are defined in (27) and $V_3 := (1/2)w^T(h^T \otimes B_2^T)(\Xi \otimes P)\delta + (1/2)\delta^T(\Xi \otimes P)(h \otimes B_2)w$.

Consider now the Hamiltonian $\mathcal{H} = \dot{V} + L(\delta^T\delta - \gamma^2 w^T w)$ L defined as in Theorem 1. Then, $\mathcal{H}$ satisfies

$$\begin{aligned}\mathcal{H} &\leq \bar{V}_1 + \bar{V}_2 + V_3 + L\left(\delta^T\delta - \gamma^2 w^T w\right)\\ &= \sum_{i\in\mathcal{F}}\left(-F_i(1-\sigma_i)\|\delta_i\|^2 - F_i\sigma_i\|\delta_i\|^2 + \frac{\bar{c}\gamma_1}{4r}\|e_i\|^2\right) + \bar{\mathcal{H}}\\ &= \sum_{i\in\mathcal{F}}\left(-F_i(1-\sigma_i)\|\delta_i\|^2 - F_i f_i\right) + \bar{\mathcal{H}} \end{aligned}\tag{39}$$

where $\bar{\mathcal{H}} \prec 0$, and F_i and f_i are defined as

$$\begin{aligned}F_i &= \frac{q\xi_i}{2} - L - \frac{\bar{c}\gamma_1 r}{4}\\ f_i &= \sigma_i\|\delta_i\|^2 - \frac{\bar{c}\gamma_1}{4rF_i}\|e_i\|^2\end{aligned}\tag{40}$$

and r be selected to guarantee

$$F_i = \frac{q\xi_i}{2} - L - \frac{\bar{c}\gamma_1 r}{4} > 0, \forall i \in \mathcal{F}. \tag{41}$$

Then, the event is triggered as long as the following condition is violated:

$$\|e_i\| \leq \pi_i\|\delta_i\|,\ \pi_i = \sqrt{\frac{4r\sigma_i}{\bar{c}\gamma_1}F_i} \tag{42}$$

which guarantees that

$$\mathcal{H} \leq -\sum_{i\in\mathcal{F}}F_i\left[(1-\sigma_i)\|\delta_i\|^2\right] \leq 0.$$

Note that the parameters satisfy

$$\frac{4r\sigma_i}{\bar{c}\gamma_1}\left(\frac{q\xi_i}{2} - L - \frac{\bar{c}\gamma_1 r}{4}\right) < \frac{4r\sigma_i}{\bar{c}\gamma_1}\left[\frac{\xi_i}{2}\left(q + \frac{\gamma_2}{\gamma^2}\right) - \frac{\bar{c}\gamma_1 r}{4}\right]$$

which is equivalent to $\pi_i < \rho_i$. Then, (42) implies that (36) holds. To guarantee both (34) and (41), r is selected as in (25). Note that as shown in Theorem 3 that follows, one needs $\pi_i \in (0, 1)$ in order to exclude Zeno behavior. Then, the condition $[(4r\sigma_i F)/(\bar{c}\gamma_1)] < 1$ should be satisfied, which is equivalent to

$$\varphi(r) := \sigma_i r^2 - \frac{4\sigma_i r}{\bar{c}\gamma_1}\left(\frac{q\xi_i}{2} - L\right) + 1 > 0.$$

Note that

$$\min_r \varphi(r) = \varphi\left(\frac{q\xi_i - 2L}{\bar{c}\gamma_1}\right) = 1 - \sigma_i\left(\frac{q\xi_i - 2L}{\bar{c}\gamma_1}\right)^2.$$

Therefore, combining the requirement of $\sigma_i \in (0, 1)$ in (37), σ_i is selected as in (26).

Therefore, the intermittent protocol (20) with the triggering condition (23) and parameters design (24)–(26) solves Problem 1. ■

Remark 3: By analyzing the two conditions of Theorem 2, the boundedness of the containment error $\delta_i(t)$ as well as its sampled version $\hat{\delta}_i(t)$ is guaranteed. This implies that the control input $u_i(t)$ in (20) of each follower also remains bounded.

Remark 4: Since the event-triggered control (20) is measurable and locally essentially bounded, the Filippov solution for (6) exists. Therefore, similar to [39], the stability of the equilibrium point of the dynamics (6) can be analyzed using differential inclusions and nonsmooth analysis [38], [40], [41]. Thus, the dynamics of the containment error δ can be written in terms of differential inclusions as [40]

$$\dot{\delta} \overset{a.e.}{\in} \mathcal{K}[(I_N \otimes A)\delta + (h \otimes B_1)u + (h \otimes B_2)w].$$

Interested readers are referred to [40] for more details about differential inclusions shown above and [39] and [41] for further applications of nonsmooth analysis in the area of MASs.

Remark 5: The intermittent containment control design in Theorem 2 depends on the sampling of $\delta_i(t)$, in contrast to the sampling of x_i in [27]. The containment error $\delta_i(t)$ can be also viewed as an extension of a combinative measurement in [19] to the case of MAS with multiple leaders. This article extends the combinative measurement-based protocol design to solve the H_∞ containment problem using both static and dynamic intermittent feedback.

B. Feasibility of the Static Intermittent Feedback

A practical issue for the implementation of intermittent feedback is that the number of triggering events does not tend to infinity in a finite amount of time, that is, the absence of Zeno behavior in Theorem 2.

Theorem 3: Suppose that the intermittent condition is designed as in Theorem 2. Then, the interevent intervals $\{t^i_{k+1} - t^i_k\}_{i=1}^{\infty}$, $\forall i \in \mathcal{F}$, are strictly positive as $k \to \infty$.

$$\frac{\mathrm{d}\|e_i(t)\|}{\mathrm{d}t} = \left\| A\left[\delta_i\left(t_k^i\right) - e_i(t)\right] - ch_{ii}B_1B_1^TP\delta_i\left(t_k^i\right) - cB_1B_1^TP\sum_{j\in\mathcal{N}_i} h_{ij}\delta_j\left(t^j_{k_j(t)}\right) + \sum_{j\in\mathcal{F}} h_{ij}B_2w_j(t)\right\|$$
$$\le \|Ae_i(t)\| + \left\|A\delta_i\left(t_k^i\right) - ch_{ii}B_1B_1^TP\delta_i\left(t_k^i\right) - cB_1B_1^TP\sum_{j\in\mathcal{N}_i} h_{ij}\delta_j\left(t^j_{k_j(t)}\right) + \sum_{j\in\mathcal{F}} h_{ij}B_2w_j(t)\right\| \le \|A\|\|e_i(t)\| + \mu_k^i \tag{47}$$

$$\mu_k^i = \max_{t\in\left[t_k^i, t_{k+1}^i\right)} \left\|A\delta_i\left(t_k^i\right) - ch_{ii}B_1B_1^TP\delta_i\left(t_k^i\right) - cB_1B_1^TP\sum_{j\in\mathcal{N}_i} h_{ij}\delta_j\left(t^j_{k_j(t)}\right) + \sum_{j\in\mathcal{F}} h_{ij}B_2w_j(t)\right\| \tag{48}$$

Proof: The intermittent condition (23) in Theorem 2 is equivalent to

$$\|e_i(t)\|^2 \le \frac{\pi_i^2\left(\|\delta_i(t)\|^2 + \|e_i(t)\|^2\right)}{1+\pi_i^2}. \tag{43}$$

Using the Young's inequality one has

$$\frac{\pi_i^2\|\delta_i(t) + e_i(t)\|^2}{2+2\pi_i^2} \le \frac{\pi_i^2\left(\|\delta_i(t)\|^2 + \|e_i(t)\|^2\right)}{1+\pi_i^2}.$$

Therefore, the sufficient condition (43) is selected as

$$\|e_i(t)\|^2 \le \frac{\pi_i^2\|\delta_i(t) + e_i(t)\|^2}{2+2\pi_i^2} = \frac{\pi_i^2\left\|\delta_i\left(t_k^i\right)\right\|^2}{2+2\pi_i^2}$$

or equivalently

$$\|e_i(t)\| \le \frac{\pi_i}{\sqrt{2+2\pi_i^2}}\left\|\delta_i\left(t_k^i\right)\right\| \triangleq s_k^i. \tag{44}$$

The evolution of $e_i(t)$ over time in $[t_k^i, t_{k+1}^i)$ satisfies

$$\frac{\mathrm{d}\|e_i(t)\|}{\mathrm{d}t} \le \frac{\left\|e_i^T(t)\right\|}{\|e_i(t)\|}\|\dot{e}_i(t)\| = \left\|\dot{\hat{\delta}}_i(t) - \dot{\delta}_i(t)\right\| \tag{45}$$

where $[(\mathrm{d}\|e_i(t)\|)/(\mathrm{d}t)]$ is the right-hand side derivative of $\|e_i(t)\|$ when $t = t_k^i$. From (18), we have that $\hat{\delta}_i(t) = \delta_i(t_k^i)$ when $t \in [t_k^i, t_{k+1}^i)$. Differentiating now $\delta_i(t)$ over the interval $[t_k^i, t_{k+1}^i)$ yields

$$\dot{\delta}_i(t) = A\delta_i(t) - ch_{ii}B_1B_1^TP\delta_i\left(t_k^i\right) - cB_1B_1^TP\sum_{j\in\mathcal{N}_i} h_{ij}\delta_j\left(t^j_{k_j(t)}\right) + \sum_{j\in\mathcal{F}} h_{ij}B_2w_j(t) \tag{46}$$

where $t^j_{k_j(t)} = \arg\max\{.t_k^j | t_k^j \le t, j \in \mathcal{N}_i\}$ denotes the latest triggering time of the follower j just before time t. Substituting (46) into (45) yields (47) and (48) (see the top of this page). Note that $e_i(t)$ is continuous on the interval $[t_k^i, t_{k+1}^i)$. Applying now the comparison principle [42] to (47) yields

$$\|e_i(t)\| \le \frac{\mu_k^i}{\|A\|}\left(e^{\|A\|\left(t-t_k^i\right)} - 1\right), t \in [t_k^i, t_{k+1}^i). \tag{49}$$

Combining the inequalities (44) and (49), when $t = t_{k+1}^i$ yields

$$\left\|e_i\left(t_{k+1}^i\right)\right\| = s_k^i \le \frac{\mu_k^i}{\|A\|}\left(e^{\|A\|\left(t_{k+1}^i - t_k^i\right)} - 1\right). \tag{50}$$

We shall now consider two cases $\forall i \in \mathcal{F}$.

1) *The Case When $\delta_i(t_k^i) \neq 0$:* Applying the triangle inequality to (48) yields

$$\mu_k^i \le \left\|A\delta_i\left(t_k^i\right)\right\| + \left\|ch_{ii}B_1B_1^TP\delta_i\left(t_k^i\right)\right\| + \left\|cB_1B_1^TP\sum_{j\in\mathcal{N}_i} h_{ij}\delta_j\left(t^j_{k_j(t)}\right)\right\| + \max_{t\in\left[t_k^i, t_{k+1}^i\right]}\left\|\sum_{j\in\mathcal{F}} h_{ij}B_2w_j(t)\right\| \triangleq \bar{\mu}_k^i$$

with $\bar{\mu}_k^i > 0$ due to the fact that $\delta_i(t_k^i) \neq 0$. Considering the facts in (50), one has

$$s_k^i \le \frac{\bar{\mu}_k^i}{\|A\|}\left(e^{\|A\|\left(t_{k+1}^i - t_k^i\right)} - 1\right)$$

which implies

$$\tau_k^i = t_{k+1}^i - t_k^i \ge \frac{1}{\|A\|}\log\left(\frac{\|A\|s_k^i}{\bar{\mu}_k^i} + 1\right).$$

Note that it is assumed that $\delta_i(t_k^i) \neq 0$. From (44), one has also $s_k^i = [(\pi_i)/(\sqrt{2+2\pi_i^2})]\|\delta_i(t_k^i)\| > 0$. Then, the argument of $log(\cdot)$ in the above inequality is strictly larger than 1. Therefore, τ_k^i is strictly positive.

2) *The Case When $\delta_i(t_k^i) = 0$:* Applying the vector norm inequality to $\delta_i(t_k^i) - \delta_i(t) = e_i(t)$ yields

$$\left|\left\|\delta_i\left(t_k^i\right)\right\| - \|\delta_i(t)\|\right| = \left|\left\|\delta_i\left(t_k^i\right)\right\| - \|-\delta_i(t)\|\right| \le \|e_i(t)\|. \tag{51}$$

From Theorem 2 and (51), the triggering condition given in (23) guarantees that

$$\left|\left\|\delta_i\left(t_k^i\right)\right\| - \|\delta_i(t)\|\right| \le \pi_i\|\delta_i(t)\|$$

which leads to

$$\frac{\left\|\delta_i\left(t_k^i\right)\right\|}{1+\pi_i} \le \|\delta_i(t)\| \le \frac{\left\|\delta_i\left(t_k^i\right)\right\|}{1-\pi_i}. \tag{52}$$

Hence, one has

$$\frac{\left\|\delta_i\left(t_k^i\right)\right\|}{\|\delta_i(t)\|} \ge 1 - \pi_i. \tag{53}$$

For the case that $\delta_i(t_k^i) = 0$, it follows from (52) that $\delta_i(t) = 0$. Then, the dynamics of the local containment error (46) yields

$$A\delta_i(t) = ch_{ii}B_1B_1^TP\delta_i\left(t_k^i\right) + cB_1B_1^TP\sum_{j\in\mathcal{N}_i} h_{ij}\delta_j\left(t^j_{k_j(t)}\right) - \sum_{j\in\mathcal{F}} h_{ij}B_2w_j(t). \tag{54}$$

Considering now (48) and (54), one has

$$\mu_k^i \leq \|A\| \left\| \delta_i\left(t_k^i\right) \right\| + \max_{t \in \left[t_k^i, t_{k+1}^i\right)} \|A\delta_i(t)\| = \|A\| \left\| \delta_i\left(t_k^i\right) \right\| + \left\| A\delta_i\left(t'\right) \right\|$$

where $t' = \arg\max_{t \in [t_k^i, t_{k+1}^i)} \|A\delta_i(t)\|$. From (53), the following holds:

$$\lim_{k \to \infty} \frac{s_k^i}{\mu_k^i} \geq \lim_{k \to \infty} \frac{\frac{\pi_i}{\sqrt{2+2\pi_i^2}} \left\| \delta_i\left(t_k^i\right) \right\|}{\|A\| \left\| \delta_i\left(t_k^i\right) \right\| + \|A\delta_i(t')\|} \geq \frac{(1-\pi_i)\pi_i}{\|A\|(2-\pi_i)\sqrt{2+2\pi_i^2}}. \tag{55}$$

Note that the inequality (50) implies

$$\tau_k^i = t_{k+1}^i - t_k^i \geq \frac{1}{\|A\|} \log\left(\frac{\|A\| s_k^i}{\mu_k^i} + 1 \right). \tag{56}$$

Finally, inserting (55) into (56) yields

$$\lim_{k \to \infty} \tau_k^i = \lim_{k \to \infty} \left(t_{k+1}^i - t_k^i\right) \geq \frac{1}{\|A\|} \log\left(\frac{\|A\| s_k^i}{\mu_k^i} + 1 \right) \geq \frac{1}{\|A\|} \log\left(\frac{(1-\pi_i)\pi_i}{(2-\pi_i)\sqrt{2+2\pi_i^2}} + 1 \right). \tag{57}$$

Note that the parameters design in (24)–(26) guarantees that $\pi_i \in (0, 1)$. Therefore, the argument of $log(\cdot)$ in last line of the above inequality is strictly larger than 1 and τ_k^i is strictly positive. ■

IV. Dynamic Intermittent Design

Note that the triggering condition (23) is static, which implies that the condition $\|e_i\| \leq \pi_i \|\delta_i\|$ is enforced for $\forall t \geq 0$. In order to further reduce the communication load, this section relaxes such requirement by introducing a dynamic intermittent mechanism.

To solve the H_∞ containment control problem, both conditions in Problem 1 are required to be satisfied. The parameters (34) and (40) in Theorem 2 satisfy

$$G_i \geq F_i \Rightarrow g_i \geq f_i. \tag{58}$$

That is, $f_i \geq 0 \Rightarrow g_i \geq 0$. Therefore, the triggering condition (23) is sufficient to solve Problem 1. Finally, the sequence of the triggering instants determined can be described $\forall i \in \mathcal{F}$ as

$$t_0^i = 0, \quad t_{k+1}^i = \inf_{t \in \mathbb{R}^+} \left\{ t > t_k^i \wedge f_i \leq 0 \right\}. \tag{59}$$

A. Dynamic Intermittent Feedback Design

To formulate the dynamic intermittent mechanism, the following internal dynamical system is considered:

$$\dot{\eta}_i = -\alpha_i \eta_i + f_i, \ \ \eta_i(0) = \eta_0^i \geq 0, \ \ \forall i \in \mathcal{F} \tag{60}$$

where f_i is defined in (40) and $\alpha_i \in \mathbb{R}^+$ is a parameter to be designed. We are now ready to present the following dynamic intermittent mechanism:

$$\eta_i(t) + \theta_i f_i \leq 0, \forall i \in \mathcal{F} \tag{61}$$

where $\theta_i \in \mathbb{R}^+$ is a design parameter. Consequently, the sequence of the triggering instants is determined by (61) $\forall i \in \mathcal{F}$, as

$$t_0^i = 0, \quad t_{k+1}^i = \inf_{t \in \mathbb{R}^+} \left\{ \left(t \in t_k^i > t_k^i\right) \wedge \left(\eta_i(t) + \theta_i f_i \leq 0\right) \right\}. \tag{62}$$

The following theorem shows that the dynamic intermittent mechanism (61) solves Problem 1.

Theorem 4: Let r, c, K be selected as in Theorem 2 and $\alpha_i, \eta(0), \theta_i \in \mathbb{R}^+$. Then, the intermittent control (20) with the event instants (62) that are being determined by (61) solves Problem 1.

Proof: Let the Lyapunov candidate for the augmented system (21) and (60) be selected as

$$\mathcal{V}(\delta, \eta) = V(\delta) + \sum_{i \in \mathcal{F}} G_i \eta_i(t) \tag{63}$$

where $V(\delta)$ is defined in Theorem 2 and G_i is defined in (34).

First, we need to show that $\eta_i \geq 0, \forall i \in \mathcal{F}$ in order to show that $\mathcal{V}$ is positive definite. Note that the dynamic triggering condition (60) and (61) guarantees $\forall i \in \mathcal{F}$

$$\eta_i(t) + \theta_i f_i \geq 0. \tag{64}$$

Since $\theta_i \in \mathbb{R}^+$, inequality (64) is equivalent to

$$f_i(t) \geq -\frac{1}{\theta_i} \eta_i(t). \tag{65}$$

Based on (60) and (65), one has

$$\dot{\eta}_i(t) \geq -\left(\alpha_i + \frac{1}{\theta_i}\right) \eta_i(t), \ \eta_i(0) \geq 0. \tag{66}$$

Applying the comparison principle [42] to (66) yields $\eta_i(t) \geq 0, \ \ \forall t \in [t_k^i, t_{k+1}^i)$ and $\forall k \in \{0, 1, 2, \ldots, \}$. Therefore, $\eta_i(t) \geq 0, \ \ \forall t \in [0, \infty)$ is guaranteed. Then, $\mathcal{V}(\delta, \eta)$ in (63) is positive definite and radially unbounded.

Next, from (37) and (58), the time derivative of $\mathcal{V}$ satisfies

$$\begin{aligned} \dot{\mathcal{V}} &= \dot{V} + \sum_{i \in \mathcal{F}} G_i(f_i - \alpha_i \eta_i) \\ &\leq \sum_{i \in \mathcal{F}} \left\{ -G_i g_i - G_i \left[(1-\sigma_i) \|\delta_i\|^2 \right] + G_i f_i - G_i \alpha_i \eta_i \right\} \\ &\leq \sum_{i \in \mathcal{F}} \left\{ -G_i g_i - G_i \left[(1-\sigma_i) \|\delta_i\|^2 \right] + G_i g_i - G_i \alpha_i \eta_i \right\} \\ &= \sum_{i \in \mathcal{F}} \left\{ -G_i \left[(1-\sigma_i) \|\delta_i\|^2 \right] - G_i \alpha_i \eta_i \right\} \leq 0. \end{aligned}$$

Note that $\sigma_i \in (0, 1), G_i > 0$, and $\eta_i \geq 0$. Therefore, $\mathcal{V}(\delta(t), \eta(t))$ decreases as $t \to \infty$ and $\delta(t) \to 0$ and $\eta(t) \to 0$. Consider the Lyapunov candidate $W(\delta, \eta) = V(\delta) + \sum_{i \in \mathcal{F}} F_i \eta_i(t)$, where $V(\delta)$ is defined in Theorem 2 and F_i is defined in (40). Similar to $\mathcal{V}, W$ also satisfies

$$\begin{aligned} &W(t) \geq 0, \dot{W}(t) \leq 0, \text{for } \forall t > 0 \\ &W(t) \to 0, \text{as} t \to \infty. \end{aligned} \tag{67}$$

Consider the Hamiltonian defined as $\mathcal{H} = \dot{W} + L(\delta^T \delta - \gamma^2 w^T w)$. Then, from (39), one has

$$\mathcal{H} = L\left(\delta^T \delta - \gamma^2 w^T w\right) + \dot{V}(\delta) + \sum_{i \in \mathcal{F}} F_i \dot{\eta}_i(t)$$

$$\leq \sum_{i\in\mathcal{F}} F_i\Big(-(1-\sigma_i)\|\delta_i\|^2 - f_i\Big) + \sum_{i\in\mathcal{F}} F_i(f_i - \alpha_i\eta_i)$$
$$= -\sum_{i\in\mathcal{F}} F_i(1-\sigma_i)\|\delta_i\|^2 - \sum_{i\in\mathcal{F}} F_i\alpha_i\eta_i \leq 0. \quad (68)$$

Based on (67) and (68), the second condition in Problem 1 is satisfied. ■

Remark 6: It is worthwhile to discuss the influence of parameters $\{\theta_i, \alpha_i, \pi_i\}$ in the dynamic triggering condition design.

1) *Effect of θ_i:* The dynamic triggering condition (61) is equivalent to
$$\left[\frac{\eta_i(t)}{\theta_i\sigma_i} + 1\right]\pi_i^2\|\delta_i(t)\|^2 \leq \|e_i(t)\|^2 \quad (69)$$
which guarantees
$$\left[\frac{\eta_i(t)}{\theta_i\sigma_i} + 1\right]\pi_i^2\|\delta_i(t)\|^2 \geq \|e_i(t)\|^2. \quad (70)$$
In (70), the left-hand side provides the upper bound of $\|e_i(t)\|^2$. Therefore, by selecting larger θ_i, the upper bound of $\|e_i(t)\|^2$ becomes smaller, which results in more frequent events. In addition, as $\theta_i \to \infty$, the above inequality becomes the static triggering condition (61). This is consistent with the discussion in [24], which shows that the static triggering condition (23) can be illustrated as a special case of the dynamic triggering condition (61) as $\theta_i \to \infty$.
2) *Effect of α_i:* To generate a larger minimum interevent interval compared to the static triggering condition, the dynamic filter with time constant $(1/\alpha_i)$ in (60) should not be too fast compared to the time constant of the signal f_i. Proper design of the dynamic filter time constant $[1/(\alpha_i)]$ can be referred to [24].
3) *Effect of π_i:* The parameter π_i appears in both static and dynamic triggering conditions, (23) and (69). In both cases, given that π_i is close to 0, implies that the event is triggered more often and hence $\hat{\delta}_i \to \delta_i$. On the other hand, by selecting larger π_i one will decrease the sampling of $\delta_i(t)$. It is true that π_i cannot exceed 1, as indicated by (57).

The use of internal dynamic variables can be found in applications where the mechanisms are equipped with internal clocks [43]. Moreover, as mentioned in Remark 6, when θ_i is selected small enough, the event-sampling frequency can be reduced significantly compared to the static event-triggering condition.

B. Feasibility of the Dynamic Intermittent Feedback

The following theorem shows that for a fixed state of the system, the interevent interval given by a dynamic intermittent mechanism is larger than the one given by the static mechanism. Then, the Zeno behavior can be avoided for the dynamic intermittent mechanism.

Theorem 5: Let $\{t_k^{s,i}\}_{k=1}^{\infty}$ and $\{t_k^{d,i}\}_{k=1}^{\infty}$ $\forall i \in \mathcal{F}$ be the intermittent time sequence determined by the static and dynamic intermittent mechanisms designed in Theorems 2 and 4, respectively. Suppose that $t_k^{s,i} = t_k^{d,i} = t_k^i$. By denoting the next intermittent time by static and dynamic intermittent mechanisms as $t_{k+1}^{s,i}$ and $t_{k+1}^{d,i}$, respectively, one has, $t_{k+1}^{d,i} \geq t_{k+1}^{s,i}$.

Proof: We will prove that by contradiction. Assume that $t_{k+1}^{d,i} < t_{k+1}^{s,i}$, $\forall i \in \mathcal{F}$. Based on the instants in (59), the following inequality is true:
$$f_i = \sigma_i\|\delta_i\|^2 - \frac{\bar{c}\gamma_1}{4rF_i}\|e_i\|^2 > 0. \quad (71)$$
Since $\alpha_i \in \mathbb{R}^+$, $\eta_i \geq 0$ and (62), one has
$$\sigma_i\|\delta_i\|^2 - \frac{\bar{c}\gamma_1}{4rF_i}\|e_i\|^2$$
$$\leq \eta_i + \theta_i\bigg(\sigma_i\|\delta_i\|^2 - \frac{\bar{c}\gamma_1}{4rF_i}\|e_i\|^2\bigg) \leq 0$$
which contradicts (71). Therefore, one concludes that $t_{k+1}^{d,i} \geq t_{k+1}^{s,i}$ which is the required result. ■

C. Discussion

The continuous communication among the agents and the constant monitoring of $\delta_i(t)$ and $e_i(t)$ in the event-triggering condition are still required. To obviate such requirement, it is desired to determine the update rules for variables $\delta_i(t)$ and $e_i(t)$. In the following equation, we only derive the calculation of $\dot{\delta}_i(t)$ because: $\dot{e}_i(t) = -\dot{\delta}_i(t)$. When there is no disturbance in (6), one has
$$\delta_i(t) = \beta_0(t) + \beta(t), t \in \big[t_k^i, t_{k+1}^i\big) \quad (72)$$
where $\beta_0(t) = \int_{t_k^i}^t A\delta_i(s)\mathrm{d}s$ and $\beta(t) = \beta_1(t) + \beta_2(t)$ with
$$\beta_1(t) = \int_{t_k^i}^t \Big[e^{A(t-s)}h_{ii}B_1u_i(s)\Big]\mathrm{d}s$$
$$= \int_{t_k^i}^t \Big[e^{A(t-s)}ch_{ii}B_1K\delta_i\big(t_k^i\big)\Big]\mathrm{d}s$$
$$\beta_2(t) = \int_{t_k^i}^t \Bigg[e^{A(t-s)}\sum_{j\in\mathcal{N}_i} ch_{ij}B_1K\delta_j(s)\Bigg]\mathrm{d}s. \quad (73)$$
Suppose that δ_j gets updated at the instants $\{t_k^i(l)\}_{l=1}^{\bar{l}}$ denoted as
$$t_k^i = t_k^i(0) < t_k^i(1) < \cdots < t_k^i(l)$$
$$< \cdots < t_k^i\big(\bar{l}\big) < t_k^i\big(\bar{l}+1\big) = t_{k+1}^i. \quad (74)$$

Therefore, for $t_k^i(0) < t \leq t_k^i(1)$, we can express $\delta_i(t)$ as
$$\delta_i(t) = \int_{t_k^i(0)}^t A\delta_i\big(t_k^i(l)\big)\mathrm{d}s$$
$$+ \int_{t_k^i(0)}^t \Big[e^{A(t-s)}ch_{ii}B_1K\delta_i\big(t_k^i\big)\Big]\mathrm{d}s$$
$$+ \int_{t_k^i(0)}^t \Bigg[e^{A(t-s)}\sum_{j\in\mathcal{N}_i} ch_{ij}B_1K\delta_j\big(t_k^i(0)\big)\Bigg]\mathrm{d}s$$
and for $t_k^i(\kappa+1) < t \leq t_k^i(\bar{l}+1)$, $\kappa = 0, 1, 2, \ldots, \bar{l}-1$, we can express $\delta_i(t)$ as
$$\delta_i(t) = \sum_{l=0}^{\kappa}\int_{t_k^i(l)}^{t_k^i(l+1)} A\delta_i\big(t_k^i(l)\big)\mathrm{d}s + \int_{t_k^i(\kappa+1)}^t A\delta_i\big(t_k^i(l)\big)\mathrm{d}s$$

This article has been accepted for inclusion in a future issue of this journal. Content is final as presented, with the exception of pagination.

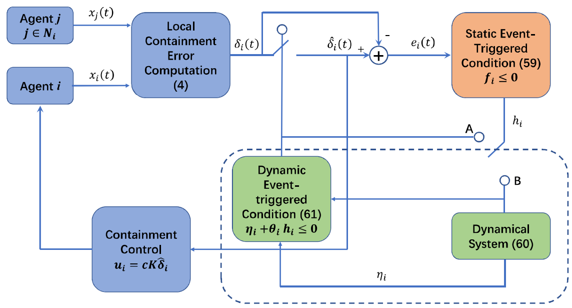

Fig. 1. Framework of the static and dynamic intermittent mechanisms.

$$
\begin{aligned}
&+\sum_{l=0}^{\kappa}\int_{t_k^i(l)}^{t_k^i(l+1)}\left[e^{A(t-s)}ch_{ii}B_1K\delta_i\left(t_k^i\right)\right]\mathrm{d}s\\
&+\int_{t_k^i(\kappa+1)}^{t}\left[e^{A(t-s)}ch_{ii}B_1K\delta_i\left(t_k^i\right)\right]\mathrm{d}s\\
&+\sum_{l=0}^{\kappa}\int_{t_k^i(l)}^{t_k^i(l+1)}\left[e^{A(t-s)}\sum_{j\in\mathcal{N}_i}ch_{ij}B_1K\delta_j\left(t_k^i(l)\right)\right]\mathrm{d}s\\
&+\int_{t_k^i(\kappa+1)}^{t}\left[e^{A(t-s)}\sum_{j\in\mathcal{N}_i}ch_{ij}B_1K\delta_j\left(t_k^i(l)\right)\right]\mathrm{d}s. \quad (75)
\end{aligned}
$$

For the case that the disturbance is nonzero, an observer-based design can be used and the above signal calculation method can be extended to an event-triggered observer design, as shown in [34]. From the above analysis, the update of $\delta_i(t)$ only depends on $\delta_j(t_k^i(l))$ and hence the continuous transmission of $\delta_i(t)$ can be avoided.

Remark 7: Given the containment error update as in (75), the monitoring of the dynamic triggering condition (61) can be implemented by a software mechanism instead of hardware. Interested readers are referred to [44] for the tradeoff between computation and communication cost. It is worth comparing dynamic and self-triggered intermittent mechanisms. The similarity between these two mechanisms is that both avoid constant monitoring of the containment error, whereas the difference lies in the event instant determination. For the self-triggered control, the next event instant is precomputed at the previous event based on system information [15], [16]. In contrast, for the dynamic intermittent feedback, the next event instant cannot be predetermined and is determined by the verification of a triggering condition, for example, (61).

We unify now the continuous feedback, and the static and dynamic intermittent feedbacks, as illustrated in Fig. 1. Option A and Option B in the hierarchical structure represent the static and the dynamic intermittent feedback, respectively. As discussed in Section II, the local containment error (4) describes the local interaction among the agents, namely, the containment error computation unit in Fig. 1. When Option A is activated, the containment error is sampled at event instants (59) and results in a static intermittent containment control, and similarly when Option B is activated, the dynamic intermittent containment control is used. Moreover, from (60) and Fig. 1, one can observe that the dynamic intermittent condition can be viewed as a filtered version of the static intermittent condition.

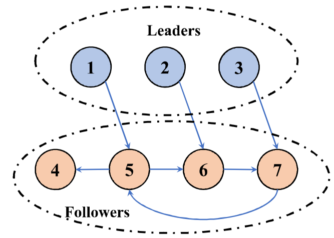

Fig. 2. Graph topology with three leaders and four followers.

V. Simulations

This section verifies the effectiveness of the proposed intermittent containment control design using three cases: continuous-feedback-based containment control, and the intermittent containment control with static and dynamic triggering conditions. Similar to existing results on containment control design for MASs with linear general high-order dynamics [7], [45]–[49], our approach makes no assumption on the order of the system dynamics. That is, although we use systems with order 2 for the simulation purpose (similar to [7] and [45]–[49]), our method can be implemented on MASs with higher-order dynamics.

Consider the MASs with three leaders and four followers connected with a communication graph as illustrated in Fig. 2, which satisfies Assumption 1. The nonsymmetric Laplacian matrix of the followers subgraph $\mathcal{F}$ is

$$
\mathcal{L}=\begin{bmatrix}1&-1&0&0\\0&2&0&-1\\0&-1&1&0\\0&0&-1&1\end{bmatrix}.
$$

Note that the directed subgraph $\mathcal{F}$ is not strongly connected, because follower 4 does not have any directed path to all other followers. The system matrices are selected as

$$
A=\begin{bmatrix}1&-3\\1&-1\end{bmatrix},\ B_1=\begin{bmatrix}0\\1\end{bmatrix},\ B_2=\begin{bmatrix}1\\1\end{bmatrix}.
$$

For the disturbance attenuation, the disturbance level is selected as $\gamma=2$ with the following disturbance being added to each follower:

$$
\begin{aligned}
&w_4=-e^{-t}\cos(t),\ w_5=-2e^{-2t}\cos(2t),\\
&w_6=-0.5e^{-1.5t}\cos(3t),\ w_7=-e^{-0.5t}\cos(4t).
\end{aligned}
$$

A. Case 1: Continuous Feedback

By following Theorem 1, the distributed containment control protocol design parameters are selected as

$$
c=1.5346,\ K=\begin{bmatrix}15.0995 & -13.0995\end{bmatrix}.
$$

The state evolutions of all the agents are depicted in Fig. 3, where the solid lines represent the envelopes formed by the state trajectories of the leader agents. The time history of the containment error is shown in Fig. 4, from which one can observe that all the containment errors approach the origin asymptotically. Fig. 5 depicts the control input of each follower. Finally, the global disturbance attenuation is shown in Fig. 6, which shows that (8) is satisfied.

This article has been accepted for inclusion in a future issue of this journal. Content is final as presented, with the exception of pagination.

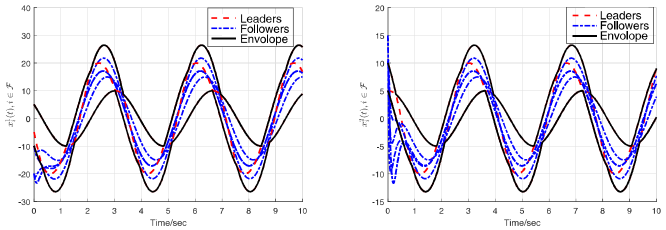

Fig. 3. Evolution of the agent's state ($x_i = [x_i^1\ x_i^2]^T$) using the continuous-feedback-based containment control.

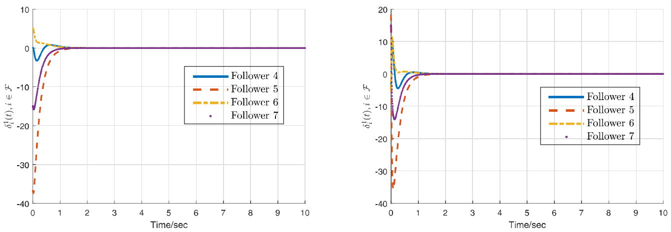

Fig. 4. Evolution of the containment error ($\delta_i = [\delta_i^1\ \delta_i^2]^T$) using the continuous-feedback-based containment control.

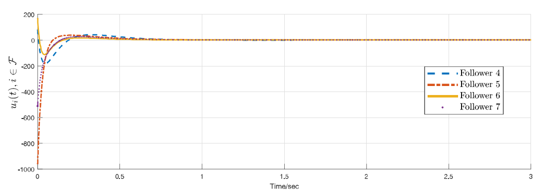

Fig. 5. Control input for all followers using the continuous-feedback-based containment control.

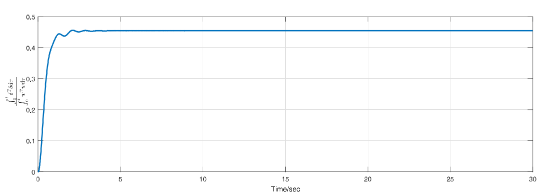

Fig. 6. Global disturbance attenuation level using the continuous-feedback-based containment control.

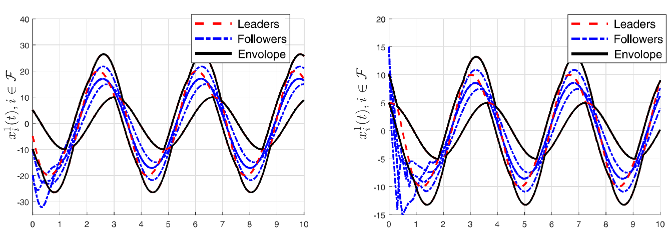

Fig. 7. Evolution of the agents' state ($x_i = [x_i^1\ x_i^2]^T$) using the static event-triggering condition.

B. Case 2: Static Event-Triggered Feedback

By following Theorem 2, we select the design parameters

$$\pi_4 = 0.51, \pi_5 = 0.52, \pi_6 = 0.53, \pi_7 = 0.54.$$

By using the event-triggered control law (20) with the static event-triggering condition (23), the state evolutions of all the agents are depicted in Fig. 7, where the solid lines represent the envelopes formed by the state trajectories of the leader

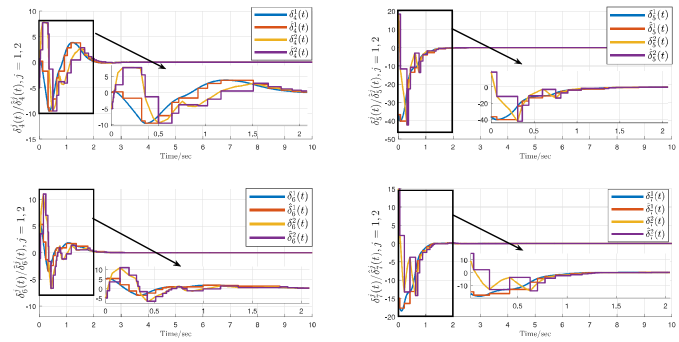

Fig. 8. Evolution of the containment error ($\delta_i = [\delta_i^1\ \delta_i^2]^T$) using the static event-triggering condition.

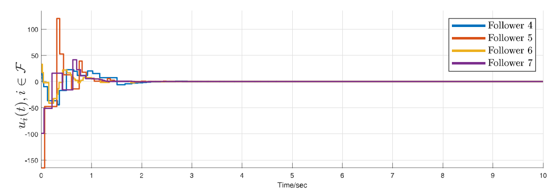

Fig. 9. Control input of all followers using the static event-triggering condition.

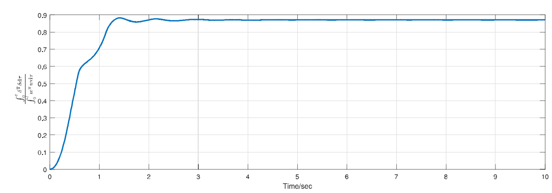

Fig. 10. Global disturbance attenuation level using the static event-triggering condition.

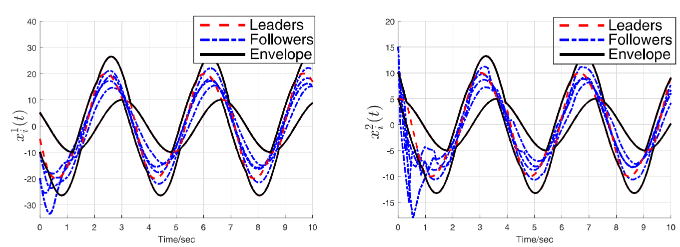

Fig. 11. Evolution of the agents' state ($x_i = [x_i^1\ x_i^2]^T$) using the dynamic event-triggering condition.

agents. The time history of the containment error with its sampled version, that is, $\delta_i(t)$ and $\hat{\delta}_i(t)$, are shown in Fig. 8. Fig. 9 depicts the control input of each follower, from which one can observe that the control input of each follower is updated independently. Finally, the global disturbance attenuation using static event-triggering condition (23) is shown in Fig. 10, which shows that the condition (8) is satisfied.

C. Case 3: Dynamic Event-Triggered Feedback

Based on Theorem 4, the dynamic intermittent parameters in (60) and (62) are selected as

$$\alpha_1 = 0.4, \alpha_2 = 0.45, \alpha_3 = 0.43, \alpha_4 = 0.42$$
$$\theta_1 = 2.8, \theta_2 = 2.7, \theta_3 = 2.6, \theta_4 = 2.9.$$

This article has been accepted for inclusion in a future issue of this journal. Content is final as presented, with the exception of pagination.

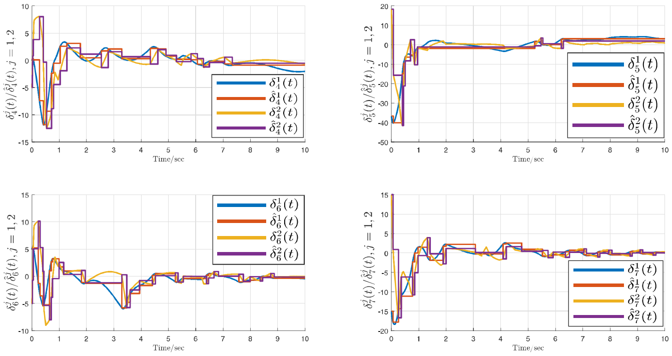

Fig. 12. Evolution of the containment error ($\delta_i = [\delta_i^1 \ \ \delta_i^2]^T$) using the dynamic event-triggering condition.

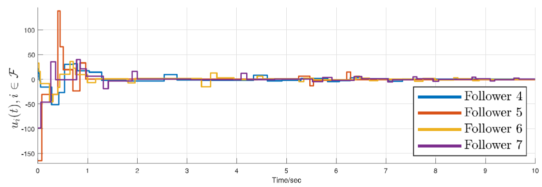

Fig. 13. Evolution of the control input of all followers using the dynamic event-triggering condition.

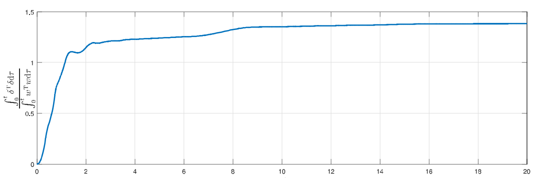

Fig. 14. Global disturbance attenuation level using the dynamic event-triggering condition.

TABLE I
COMMUNICATION BANDWIDTH COMPARISON

Triggering Case	Number of triggering instants			
	Follower 4	Follower 5	Follower 6	Follower 7
Case 2	77	76	74	68
Case 3	28	12	33	32

By using the event-triggered control law (20) with the dynamic event-triggering condition (61), the state evolutions of all the agents are depicted in Fig. 11, where the solid lines represent the envelopes formed by the state trajectories of the leader agents. The time history of the containment error with its sampled version, that is, $\delta_i(t)$ and $\hat{\delta}_i(t)$, are shown in Fig. 12. Fig. 13 depicts the control input of each follower. Finally, the global disturbance attenuation using static event-triggering condition (61) is shown in Fig. 14, which shows that the condition (8) is satisfied. We observe that the state trajectories of all the followers converge to the convex hull spanned by the leaders. The evolution of the gap $e_i(t)$ for the containment error $\delta_i(t)$ and its triggering threshold using both triggering conditions (23) and (61), are also presented in Fig. 15. It can be shown that all agents are triggered independently. In both cases, both the gap $e_i(t)$ and its threshold approach the origin, implying that the containment target is achieved. In addition, from Fig. 15, one can observe that the threshold in the dynamic

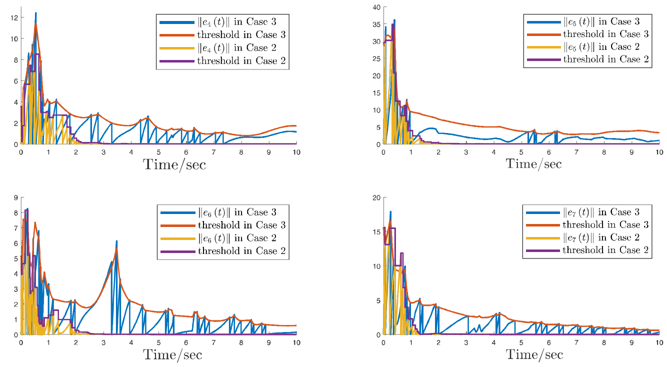

Fig. 15. Evolution of each agents' error with respect to the threshold for cases 2 and 3.

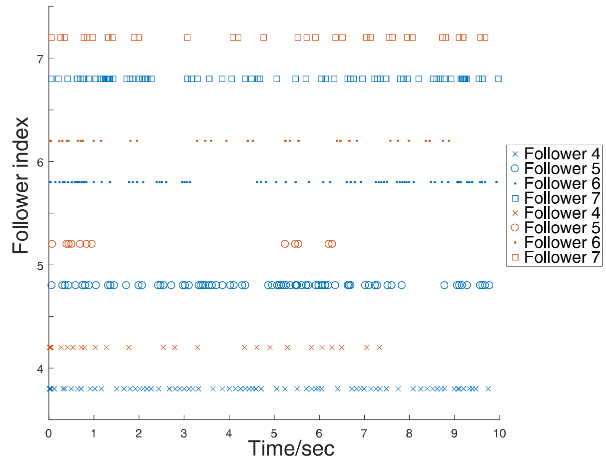

Fig. 16. Triggering instants of the agents for cases 2 and 3.

triggering condition is larger than that in the static triggering condition and the event-triggering instants in the dynamic triggering case are less than those in the static triggering case. The event-triggering instants using static and dynamics event-triggering conditions are shown in Fig. 16. The number of event-triggering instants of each follower in cases 2 and 3 are given in Table I. Compared to the static mechanism, the dynamic intermittent mechanism reduces the communication load significantly.

VI. CONCLUSION

This article investigated the distributed intermittent containment control design of linear MAS. Two different types of intermittent containment control protocols were presented, namely, a static and a dynamic intermittent distributed protocol. The closed-loop stability of the equilibrium point and the Zeno-free behavior are thoroughly analyzed. Moreover, a unified framework is given to illustrate the relationship between the static and the dynamic intermittent protocols. Simulation results are presented to show the efficacy of the presented approach and a performance comparison of the dynamic over the static intermittent mechanism in terms of the sampling frequency.

REFERENCES

[1] J. A. Fax and R. M. Murray, "Information flow and cooperative control of vehicle formations," *IEEE Trans. Autom. Control*, vol. 49, no. 9, pp. 1465–1476, Sep. 2004.

[2] H. Zhang, T. Feng, G.-H. Yang, and H. Liang, "Distributed cooperative optimal control for multiagent systems on directed graphs: An inverse optimal approach," *IEEE Trans. Cybern.*, vol. 45, no. 7, pp. 1315–1326, Jul. 2015.

[3] W. Ren and Y. Cao, *Distributed Coordination of Multi-Agent Networks: Emergent Problems, Models, and Issues*. New York, NY, USA: Springer, 2010.

[4] A. Bidram, F. L. Lewis, and A. Davoudi, "Distributed control systems for small-scale power networks: Using multiagent cooperative control theory," *IEEE Control Syst. Mag.*, vol. 34, no. 6, pp. 56–77, Dec. 2014.

[5] Z. Kan, J. R. Klotz, E. L. Pasiliao, Jr., and W. E. Dixon, "Containment control for a social network with state-dependent connectivity," *Automatica*, vol. 56, pp. 86–92, Jun. 2015.

[6] L. Ding, Q.-L. Han, X. Ge, and X.-M. Zhang, "An overview of recent advances in event-triggered consensus of multiagent systems," *IEEE Trans. Cybern.*, vol. 48, no. 4, pp. 1110–1123, Apr. 2018.

[7] H. Haghshenas, M. A. Badamchizadeh, and M. Baradarannia, "Containment control of heterogeneous linear multi-agent systems," *Automatica*, vol. 54, pp. 210–216, Apr. 2015.

[8] Y. Yang, H. Modares, D. C. Wunsch, and Y. Yin, "Optimal containment control of unknown heterogeneous systems with active leaders," *IEEE Trans. Control Syst. Technol.*, vol. 27, no. 3, pp. 1228–1236, May 2019.

[9] X. Dong, Z. Shi, G. Lu, and Y. Zhong, "Formation-containment analysis and design for high-order linear time-invariant swarm systems," *Int. J. Robust Nonlin. Control*, vol. 25, no. 17, pp. 3439–3456, 2015.

[10] X. Dong, Q. Li, Z. Ren, and Y. Zhong, "Output formation-containment analysis and design for general linear time-invariant multi-agent systems," *J. Frankl. Inst.*, vol. 353, no. 2, pp. 322–344, 2016.

[11] P. Tabuada, "Event-triggered real-time scheduling of stabilizing control tasks," *IEEE Trans. Autom. Control*, vol. 52, no. 9, pp. 1680–1685, Sep. 2007.

[12] X. Ge, Q.-L. Han, D. Ding, X.-M. Zhang, and B. Ning, "A survey on recent advances in distributed sampled-data cooperative control of multi-agent systems," *Neurocomputing*, vol. 275, pp. 1684–1701, Jan. 2018.

[13] W. Hu, L. Liu, and G. Feng, "Output consensus of heterogeneous linear multi-agent systems by distributed event-triggered/self-triggered strategy," *IEEE Trans. Cybern.*, vol. 47, no. 8, pp. 1914–1924, Aug. 2017.

[14] Y. Yang, K. G. Vamvoudakis, H. Ferraz, and H. Modares, "Dynamic intermittent Q-learning-based model-free suboptimal co-design of L_2-stabilization," *Int. J. Robust Nonlin. Control*, vol. 29, no. 9, pp. 2673–2694, 2019.

[15] Y. Wang, W. X. Zheng, and H. Zhang, "Dynamic event-based control of nonlinear stochastic systems," *IEEE Trans. Autom. Control*, vol. 62, no. 12, pp. 6544–6551, Dec. 2017.

[16] X. Yi, K. Liu, D. V. Dimarogonas, and K. H. Johansson, "Dynamic event-triggered and self-triggered control for multi-agent systems," *IEEE Trans. Autom. Control*, vol. 64, no. 8, pp. 3300–3307, Aug. 2019. doi: 10.1109/TAC.2018.2874703.

[17] G. Wen, Z. Duan, W. Yu, and G. Chen, "Consensus in multi-agent systems with communication constraints," *Int. J. Robust Nonlin. Control*, vol. 22, no. 2, pp. 170–182, 2012.

[18] G. Wen, Z. Duan, G. Chen, and W. Yu, "Consensus tracking of multi-agent systems with Lipschitz-type node dynamics and switching topologies," *IEEE Trans. Circuits Syst. I, Reg. Papers*, vol. 61, no. 2, pp. 499–511, Feb. 2013.

[19] Y. Fan, G. Feng, Y. Wang, and C. Song, "Distributed event-triggered control of multi-agent systems with combinational measurements," *Automatica*, vol. 49, no. 2, pp. 671–675, 2013.

[20] W. Hu, L. Liu, and G. Feng, "Consensus of linear multi-agent systems by distributed event-triggered strategy," *IEEE Trans. Cybern.*, vol. 46, no. 1, pp. 148–157, Jan. 2016.

[21] D. Yang, W. Ren, X. Liu, and W. Chen, "Decentralized event-triggered consensus for linear multi-agent systems under general directed graphs," *Automatica*, vol. 69, pp. 242–249, Jul. 2016.

[22] D. V. Dimarogonas, E. Frazzoli, and K. H. Johansson, "Distributed event-triggered control for multi-agent systems," *IEEE Trans. Autom. Control*, vol. 57, no. 5, pp. 1291–1297, May 2012.

[23] X. Ge and Q.-L. Han, "Distributed formation control of networked multi-agent systems using a dynamic event-triggered communication mechanism," *IEEE Trans. Ind. Electron.*, vol. 64, no. 10, pp. 8118–8127, Oct. 2017.

[24] A. Girard, "Dynamic triggering mechanisms for event-triggered control," *IEEE Trans. Autom. Control*, vol. 60, no. 7, pp. 1992–1997, Jul. 2015.

[25] Q. Jiao, H. Modares, F. L. Lewis, S. Xu, and L. Xie, "Distributed $\mathcal{L}_2$-gain output-feedback control of homogeneous and heterogeneous systems," *Automatica*, vol. 71, pp. 361–368, Sep. 2016.

[26] W. Zhang, Y. Tang, Y. Liu, and J. Kurths, "Event-triggering containment control for a class of multi-agent networks with fixed and switching topologies," *IEEE Trans. Circuits Syst. I, Reg. Papers*, vol. 64, no. 3, pp. 619–629, Mar. 2017.

[27] T.-H. Cheng, Z. Kan, J. R. Klotz, J. M. Shea, and W. E. Dixon, "Decentralized event-triggered control of networked systems—Part 2: Containment control," in *Proc. Amer. Control Conf. (ACC)*, Jul. 2015, pp. 5444–5448.

[28] A. Das and F. L. Lewis, "Distributed adaptive control for synchronization of unknown nonlinear networked systems," *Automatica*, vol. 46, no. 12, pp. 2014–2021, 2010.

[29] Z. Meng, Z. Zhao, and Z. Lin, "On global leader-following consensus of identical linear dynamic systems subject to actuator saturation," *Syst. Control Lett.*, vol. 62, no. 2, pp. 132–142, 2013.

[30] S. Boyd and L. Vandenberghe, *Convex Optimization*. New York, NY, USA: Cambridge Univ. Press, 2004.

[31] H. Zhang, Z. Li, Z. Qu, and F. L. Lewis, "On constructing Lyapunov functions for multi-agent systems," *Automatica*, vol. 58, pp. 39–42, Aug. 2015.

[32] G. Wen, W. Yu, Z. Li, X. Yu, and J. Cao, "Neuro-adaptive consensus tracking of multiagent systems with a high-dimensional leader," *IEEE Trans. Cybern.*, vol. 47, no. 7, pp. 1730–1742, Jul. 2017.

[33] X. Dong, F. Meng, Z. Shi, G. Lu, and Y. Zhong, "Output containment control for swarm systems with general linear dynamics: A dynamic output feedback approach," *Syst. Control Lett.*, vol. 71, pp. 31–37, Sep. 2014.

[34] H. Zhang, J. Han, Y. Wang, and H. Jiang, "H_∞ consensus for linear heterogeneous multiagent systems based on event-triggered output feedback control scheme," *IEEE Trans. Cybern.*, vol. 49, no. 6, pp. 2268–2279, Jul. 2019.

[35] F. L. Lewis, D. Vrabie, and V. L. Syrmos, *Optimal Control*. Hoboken, NJ, USA: Wiley, 2012.

[36] Z. Li, Z. Duan, W. Ren, and G. Feng, "Containment control of linear multi-agent systems with multiple leaders of bounded inputs using distributed continuous controllers," *Int. J. Robust Nonlin. Control*, vol. 25, no. 13, pp. 2101–2121, 2015.

[37] P. Wang and Y. Jia, "Robust H_∞ containment control for uncertain multi-agent systems with inherent nonlinear dynamics," *Int. J. Syst. Sci.*, vol. 47, no. 5, pp. 1073–1083, 2016.

[38] D. Shevitz and B. Paden, "Lyapunov stability theory of nonsmooth systems," *IEEE Trans. Autom. Control*, vol. 39, no. 9, pp. 1910–1914, Sep. 1994.

[39] Z. Li, X. Liu, W. Ren, and L. Xie, "Distributed tracking control for linear multiagent systems with a leader of bounded unknown input," *IEEE Trans. Autom. Control*, vol. 58, no. 2, pp. 518–523, Feb. 2013.

[40] B. E. Paden and S. S. Sastry, "A calculus for computing Filippov's differential inclusion with application to the variable structure control of robot manipulators," *IEEE Trans. Circuits Syst.*, vol. 34, no. 1, pp. 73–82, Jan. 1987.

[41] Y. Cao, D. Stuart, W. Ren, and Z. Meng, "Distributed containment control for multiple autonomous vehicles with double-integrator dynamics: Algorithms and experiments," *IEEE Trans. Control Syst. Technol.*, vol. 19, no. 4, pp. 929–938, Jul. 2011.

[42] H. K. Khalil, *Nonlinear Systems*. Englewood Cliffs, NJ, USA: Prentice-Hall, 1996.

[43] M. Mazo, A. Anta, and P. Tabuada, "An ISS self-triggered implementation of linear controllers," *Automatica*, vol. 46, no. 8, pp. 1310–1314, 2010.

[44] S. Akashi, H. Ishii, and A. Cetinkaya, "Self-triggered control with tradeoffs in communication and computation," *Automatica*, vol. 94, pp. 373–380, Aug. 2018.

[45] H. Liu, L. Cheng, M. Tan, and Z.-G. Hou, "Containment control of continuous-time linear multi-agent systems with aperiodic sampling," *Automatica*, vol. 57, pp. 78–84, Jul. 2015.

[46] J. Mei, W. Ren, and G. Ma, "Distributed containment control for Lagrangian networks with parametric uncertainties under a directed graph," *Automatica*, vol. 48, no. 4, pp. 653–659, 2012.

[47] Q. Xiao, F. L. Lewis, and Z. Zeng, "Containment control for multiagent systems under two intermittent control schemes," *IEEE Trans. Autom. Control*, vol. 64, no. 3, pp. 1236–1243, Mar. 2019.

[48] D. Wang, D. Wang, and W. Wang, "Necessary and sufficient conditions for containment control of multi-agent systems with time delay," *Automatica*, vol. 103, pp. 418–423, May 2019.

[49] W. Chen, D. Ding, X. Ge, Q.-L. Han, and G. Wei, "H_∞ containment control of multiagent systems under event-triggered communication scheduling: The finite-horizon case," *IEEE Trans. Cybern.*, to be published.

Yongliang Yang (S'16–M'18) received the B.S. degree from Hebei University, Baoding, China, in 2011, and the Ph.D. degree from the University of Science and Technology Beijing (USTB), Beijing, China, in 2017.

He was a Visiting Scholar with the Missouri University of Science and Technology, Rolla, MO, USA, from 2015 to 2017, sponsored by China Scholarship Council. He is currently an Assistant Professor with USTB. His current research interests include adaptive optimal control, distributed optimization and control, and cyber-physical systems.

Dr. Yang was a recipient of the Best Ph.D. Dissertation of China Association of Artificial Intelligence, the Best Ph.D. Dissertation of USTB, the Chancellors Scholarship in USTB, and the Excellent Graduates Awards in Beijing. He also serves as the Reviewer of several international journals and conferences, including *Automatica*, the IEEE TRANSACTIONS ON AUTOMATIC CONTROL, the IEEE TRANSACTIONS ON CYBERNETICS, and the IEEE TRANSACTIONS ON NEURAL NETWORKS AND LEARNING SYSTEMS.

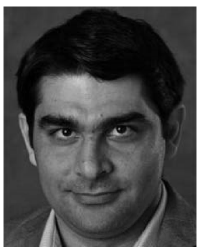

Hamidreza Modares (M'15) received the B.S. degree from the University of Tehran, Tehran, Iran, in 2004, the M.S. degree from the Shahrood University of Technology, Shahrood, Iran, in 2006, and the Ph.D. degree from the University of Texas at Arlington, Arlington, TX, USA, in 2015.

He was a Faculty Research Associate with the University of Texas at Arlington from 2015 to 2016, and an Assistant Professor with the Missouri University of Science and Technology, Rolla, MO, USA, from 2016 to 2018. He is currently an Assistant Professor with the Mechanical Engineering Department, Michigan State University, East Lansing, MI, USA. His current research interests include cyber-physical systems, reinforcement learning, distributed control, robotics, and machine learning.

Dr. Modares was a recipient of the Best Paper Award from the 2015 IEEE International Symposium on Resilient Control Systems. He is an Associate Editor of the IEEE TRANSACTIONS ON NEURAL NETWORKS AND LEARNING SYSTEMS.

Kyriakos G. Vamvoudakis (SM'15) was born in Athens, Greece. He received the Diploma (a five-year degree, equivalent to a master of science) degree (with Highest Hons.) in electronic and computer engineering from the Technical University of Crete, Chania, Greece, in 2006, and the M.S. and Ph.D. degrees in electrical engineering from the University of Texas at Arlington, Arlington, TX, USA, in 2008 and 2011, respectively.

From 2012 to 2016, he was a Project Research Scientist with the Center for Control, Dynamical Systems and Computation, University of California at Santa Barbara, Santa Barbara, CA, USA. He is currently an Assistant Professor with the Kevin T. Crofton Department of Aerospace and Ocean Engineering, Virginia Tech, Blacksburg, VA, USA. He has coauthored 1 patent, over 90 technical publications, and 2 books. His current research interests include game-theoretic control, network security, smart grid, and multiagent optimization.

Dr. Vamvoudakis was a recipient of several international awards, including the International Neural Network Society Young Investigator Award in 2016, the Best Paper Award for Autonomous/Unmanned Vehicles at the 27th Army Science Conference in 2010, the Best Presentation Award at the World Congress of Computational Intelligence in 2010, and the Best Researcher Award from the Automation and Robotics Research Institute in 2011. He is currently an Associate Editor of the *Journal of Optimization Theory and Applications* and *Control Theory and Technology*, a Registered Electrical/Computer Engineer (PE), and a member of the Technical Chamber of Greece.

Yixin Yin (M'07) received the B.S., M.S., and Ph.D. degrees from the University of Science and Technology Beijing (USTB), Beijing, China, in 1982, 1984, and 2002, respectively.

He was a Visiting Scholar with several universities in Japan, including the University of Tokyo, Tokyo, Japan; the Kyushu Institute of Technology, Kitakyushu, Japan; Kanagawa University, Yokohama, Japan; Chiba University, Chiba, Japan; and the Muroran Institute of Technology, Muroran, Japan. He is currently a Professor with the School of Automation and Electrical Engineering, USTB, where he served as the Dean of the School of the Information Engineering from 2000 to 2011 and the School of Automation and Electrical Engineering from 2011 to 2017. His current research interests include modeling and control of complex industrial processes, computer-aided design of control system, intelligent control, and artificial life.

Prof. Yin was a recipient of several national awards, including the Outstanding Young Educator in 1993, the Award of Science and Technology Progress in Education in 1994, the Award of National Science and Technology Progress in 1995, the Special Allowance of the State Council in 1994, the Best Paper of Japanese Acoustical Society in 1999, and the Award of Metallurgical Science and Technology in 2014. He is a fellow of the China Association of Artificial Intelligence, and a member of the Chinese Society for Metals and the Chinese Association of Automation.

Donald C. Wunsch, II (F'05) received the B.S. degree in applied mathematics from the University of New Mexico, Albuquerque, NM, USA, in 1984, the M.S. degree in applied mathematics and the Ph.D. degree in electrical engineering from the University of Washington, Seattle, WA, USA, in 1987 and 1991, respectively, and the Executive M.B.A. degree from Washington University in St. Louis, St. Louis, MO, USA, in 2006.

He attended the Jesuit Core Honors Program with Seattle University, Seattle, WA, USA. He was with Texas Tech University, Lubbock, TX, USA; Boeing, Seattle, WA, USA; Rockwell International, Albuquerque, NM, USA; and International Laser Systems, Albuquerque, NM, USA. He is currently the Mary K. Finley Missouri Distinguished Professor with the Missouri University of Science and Technology (Missouri S&T), Rolla, MO, USA, where he is also the Director of the Applied Computational Intelligence Laboratory, a multidisciplinary research group. His current research interests include clustering/unsupervised learning; biclustering; adaptive resonance and adaptive dynamic programming architectures, hardware, and applications; neurofuzzy regression; autonomous agents; games; and bioinformatics.

Dr. Wunsch, II, was a recipient of the NSF CAREER Award, the 2015 INNS Gabor Award, and the 2019 Ada Lovelace Service Award. He has produced 21 Ph.D. recipients in computer engineering, electrical engineering, systems engineering, and computer science. He is an International Neural Networks Society (INNS) Fellow and the INNS President. He served as the IJCNN General Chair, and on several boards, including the St. Patricks School Board, the IEEE Neural Networks Council, the INNS, and the University of Missouri Bioinformatics Consortium, and the Chair of the Missouri S&T Information Technology and Computing Committee as well as the Student Design and Experiential Learning Center Board.